Selecting climate change scenarios using impact-relevant sensitivities

Citation	Vano, J. A., Kim, J. B., Rupp, D. E., & Mote, P. W. (2015). Selecting climate change scenarios using impact-relevant sensitivities. Geophysical Research Letters, 42(13), 5516-5525. doi:10.1002/2015GL063208
DOI	10.1002/2015GL063208
Publisher	John Wiley & Sons Ltd.
Version	Version of Record
Terms of Use	http://cdss.library.oregonstate.edu/sa-termsofuse

AGU PUBLICATIONS

Geophysical Research Letters

RESEARCH LETTER
10.1002/2015GL063208

Key Points:
- Impact-relevant sensitivities are employed to customize GCM selection
- Isolines in ΔP-ΔT space indicate streamflow and vegetation carbon change
- Approach provides quick estimates of the range of impacts for future projections

Supporting Information:
- Figures S1–S3, Tables S1–S6, and Text S1

Correspondence to:
J. A. Vano,
jvano@coas.oregonstate.edu

Citation:
Vano, J. A., J. B. Kim, D. E. Rupp, and P. W. Mote (2015), Selecting climate change scenarios using impact-relevant sensitivities, *Geophys. Res. Lett.*, *42*, 5516–5525, doi:10.1002/2015GL063208.

Received 22 JAN 2015
Accepted 11 JUN 2015
Accepted article online 16 JUN 2015
Published online 7 JUL 2015

Selecting climate change scenarios using impact-relevant sensitivities

Julie A. Vano[1], John B. Kim[2], David E. Rupp[1], and Philip W. Mote[1]

[1]Oregon Climate Change Research Institute, College of Earth, Ocean, and Atmospheric Sciences, Oregon State University, Corvallis, Oregon, USA, [2]Pacific Northwest Research Station and Western Wildland Environmental Threat Assessment Center, U.S. Forest Service, Prineville, Oregon, USA

Abstract Climate impact studies often require the selection of a small number of climate scenarios. Ideally, a subset would have simulations that both (1) appropriately represent the range of possible futures for the variable/s most important to the impact under investigation and (2) come from global climate models (GCMs) that provide plausible results for future climate in the region of interest. We demonstrate an approach to select a subset of GCMs that incorporates both concepts and provides insights into the range of climate impacts. To represent how an ecosystem process responds to projected future changes, we methodically sample, using a simple sensitivity analysis, how an ecosystem variable responds locally to projected regional temperature and precipitation changes. We illustrate our approach in the Pacific Northwest, focusing on (a) changes in streamflow magnitudes in critical seasons for water management and (b) changes in annual vegetation carbon.

1. Introduction

Increasingly, natural resource management agencies and others are seeking ways to incorporate climate change projections into their long-term planning (*Adger et al*. [2005], *U.S. Environmental Protection Agency* [2009], *Means et al*. [2010], *Adelsman and Ekrem* [2012], *Harding et al*. [2012], *U.S. Fish and Wildlife Service* [2013], *U.S. Bureau of Reclamation* (*USBR*) [2013], *Weaver et al*. [2013], and many more). In fact, U.S. federal agencies are required to consider climate change risks and vulnerabilities on operations through Presidential Executive Order 13514. Simultaneously, climate modelers are generating more climate change information. For example, global climate model (GCM) output from the Coupled Model Intercomparison Project Phase 5 (CMIP5) contains more than 35 GCMs simulating both historical and future climates with 1–10 realizations for each model and four different scenarios of future greenhouse gas concentrations prescribed through Representative Concentration Pathways (RCPs) [*Taylor et al*., 2012] (http://cmip-pcmdi.llnl.gov/cmip5).

The use of climate data ranges from qualitative descriptions to computationally intensive impact models that use downscaled climate model outputs directly. In impact model assessments, many academic researchers and management agencies lack the capacity to ingest all available climate scenarios into their planning process, especially when other types of future projections (e.g., changes in demographics, land use, and economic conditions) are also being considered. Instead, they select a subset of projections and are seeking objective, defensible choices for their publicly scrutinized decision-making [*Snover et al*., 2013]. Preferably, a subset of GCM simulations should (1) represent the range of possible futures for the variables most important to the impact under investigation and (2) favor models that adequately simulate historical climate, thus enhancing the plausibility of results for future simulations in the region of interest. In some evaluations the full range of impacts is desired, while other evaluations only want the worst or central case. The approach described here enables the user to select which of these is appropriate for the risk tolerance and decision criteria of the particular evaluation.

Studies have offered guidance on GCM selection [*Mote et al*., 2011; *Snover et al*., 2013] and ways to rank GCM performance at the regional scale [*Giorgi and Mearns*, 2002; *Brekke et al*., 2008; *Pitman and Perkins*, 2008; *Pierce et al*., 2009; *Mote and Salathé*, 2010; *Rupp et al*., 2013] with the aim of selecting or weighting models. In this paper, building on such guidance, we demonstrate a technique that employs a quantitative, objective approach that aids selection, especially in situations when only a small number of GCMs can be selected.

Specifically, we present an approach that shows where GCM projections lie on an impacts spectrum using a sensitivity analysis as outlined in *Vano and Lettenmaier* [2014] and accounts for GCM performance for the

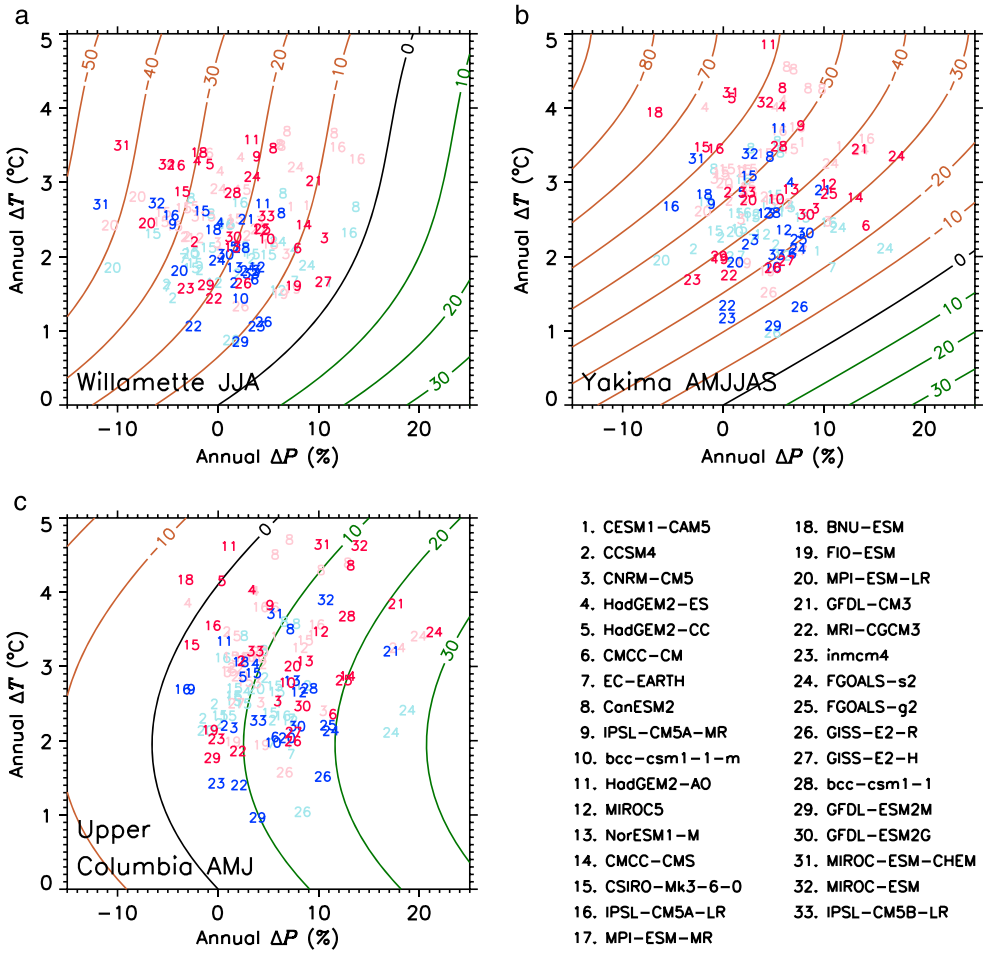

Figure 1. GCM selection plots for seasonal streamflow change. Isolines, calculated using results shown in Figures 3a and 3b, represent constant change in streamflow for three watersheds: (a) Willamette, (b) Yakima, and (c) Upper Columbia. GCM positions in ΔP-ΔT space are identified with performance ranking numbers. Blue numbers are RCP4.5, and red numbers are RCP8.5, where lighter numbers indicate multiple runs for the same GCM. For values, see Tables S1 and S2.

Pacific Northwest (PNW), USA, as in *Rupp et al.* [2013]. This approach is computationally efficient and, by estimating one or two key impact variables, provides a richer framework than just ranges of GCM-derived changes in temperature (T) and precipitation (P). It parallels the vulnerability assessment, or stress test, promoted by *Brown and Wilby* [2012] as it is a "bottom-up meets top-down" approach that emphasizes the impact of concern (ecosystem variable) in the GCM selection process. We demonstrate the technique by evaluating how climate change will affect seasonal streamflow magnitudes and annual vegetation carbon stocks in diverse geographic settings across the PNW. In this evaluation, we focus on changes in the 30 year mean, which does not capture the frequency of individual events (e.g., floods and droughts) and therefore cannot be used to select GCMs that span the range of extreme events.

2. Methods

2.1. ΔT_{GCM} and ΔP_{GCM}

Projections of regional climate change were calculated from simulated values of monthly mean T and P from 33 GCMs for which data were available for the CMIP5 *historical* (1850–2005) and the RCP4.5 and RCP8.5 (2006–2100) experiments. Multiple runs were available for some GCMs, for a total of 142 simulations. The historical experiment applied both observed anthropogenic and natural forcings, while the RCP4.5 and RCP8.5 experiments applied plausible future forcings [*Meinshausen et al.*, 2011; *Taylor et al.*, 2012]. Data from each GCM were regridded to a common 1° longitude-latitude resolution

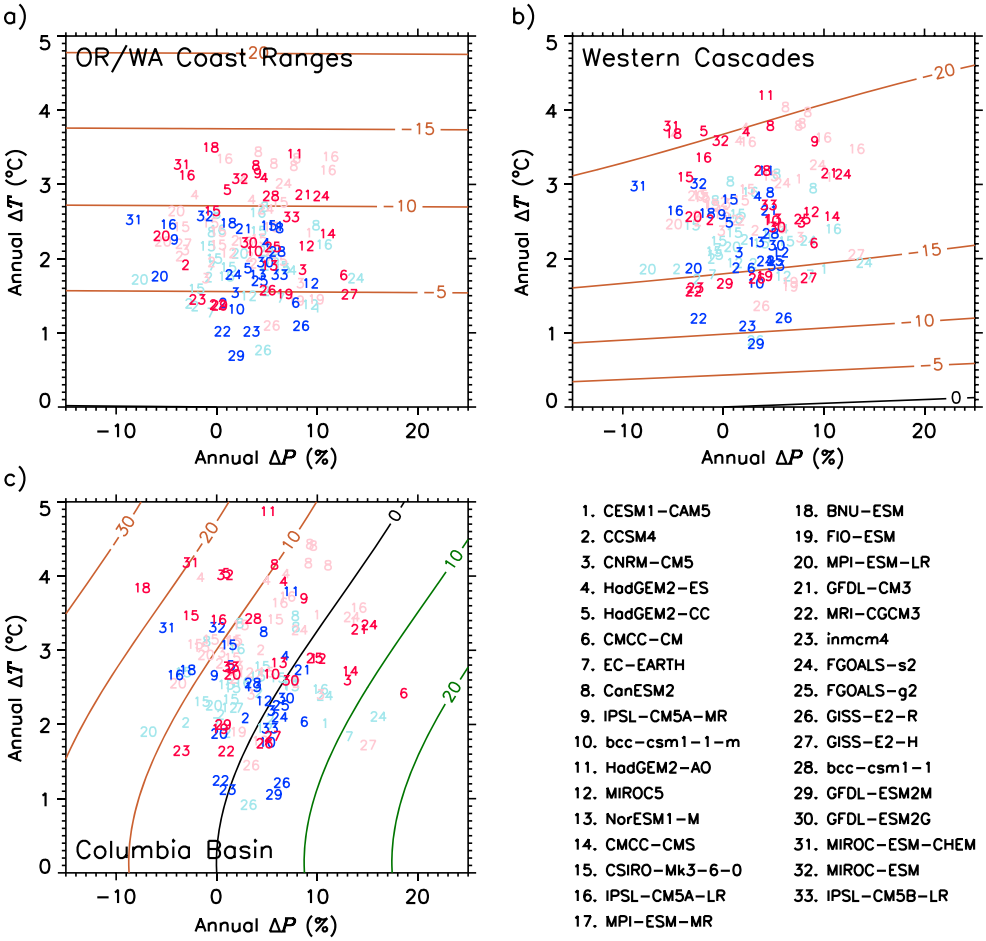

Figure 2. GCM selection plots for vegetation carbon change. Similar to Figure 1, but isolines, calculated using results shown in Figures 3c and 3d, represent constant change in vegetation carbon for three ecoregions: (a) OR/WA Coast Ranges, (b) Western Cascades, and (c) Columbia Basin. For values, see Tables S3 and S4.

grid using inverse distance weighting of four nearest neighbors, and changes in T and P through time (denoted ΔT_{GCM} and ΔP_{GCM}) were calculated as the difference in *annual* mean values over a future 30 year period (2041–2070) and reference historical period (1970–1999). The change was further averaged spatially over grids that encompassed the six study areas (see Figure S1 in the supporting information for map). The ranges of ΔT_{GCM} and ΔP_{GCM} from all GCM runs (Figures 1 and 2) were used to determine the span of T and P perturbations used to calculate impact-relevant sensitivities. In this analysis, we used *annual* (versus *seasonal*) ΔT and ΔP values as evaluations (see Text S1) indicated that this simplification had little influence on the overall response.

2.2. Impact-Relevant Sensitivities

To identify GCM simulations that appropriately represent the range of an identified impact, we used the concept of hydrologic sensitivities, which we adapt also to investigate vegetation carbon sensitivities. *Vano and Lettenmaier* [2014] showed how simple perturbation experiments of T and P can be employed with good accuracy to estimate how streamflow responds to ΔT_{GCM} and ΔP_{GCM}. We conducted similar experiments to assess sensitivity of streamflow in three watersheds in management-relevant seasons and sensitivity of vegetation carbon in three ecoregions. More specifically, we calculated temperature sensitivities (S), defined as the percent change in the impact (ΔI) per °C increase in temperature (ΔT):

$$S = \Delta I / \Delta T \quad (1)$$

and precipitation elasticities (ε), defined as the percent change in the impact (ΔI) per percent change in precipitation (ΔP):

$$\varepsilon = \Delta I / \Delta P \tag{2}$$

We calculated seasonal and annual S and ε values using T and P perturbations that span the range of annual mean ΔT_{GCM} and ΔP_{GCM}.

Assuming that changes in ΔI from changes in T and P are additive and have no interactions, we estimate ΔI as

$$\Delta I = S(\Delta T)\Delta T + \varepsilon(\Delta P)\Delta P \tag{3}$$

where S is a function of ΔT and ε is a function of ΔP. Subscripts for ΔI, S, and ε designate either streamflow (q) or vegetation carbon (c). In this study, we represent $S(\Delta T)$ with a quadratic equation and $\varepsilon(\Delta P)$ with a constant because our analysis showed that in our areas of interest S varied strongly with changing ΔT, whereas ε was relatively constant with changing ΔP.

Using sensitivity values, described in sections 2.2.1 and 2.2.2, and equation (3) for each region and impact (I_q or I_c), we placed isolines of constant ΔI on a plot of ΔT versus ΔP. Such plots represent the response surface of future changes and can be used to identify where GCM projections lie on a spectrum of an impact (e.g., streamflow change) and guide selection of best performing GCMs (described in section 2.3) that have the highest, middle, and lowest values for that impact.

2.2.1. Hydrologic Sensitivities

We calculated hydrologic sensitivities (S_q, ε_q) in different seasons using the variable infiltration capacity (VIC) hydrologic model [*Liang et al*., 1994] configured for the PNW as in *Vano et al*. [2015]. Spatially uniform T and P perturbations were applied independently to every day of a historical data set (1970–2004) [*Elsner et al*., 2010; *Hamlet et al*., 2013] used as meteorological forcings for the VIC model. S_q and ε_q were calculated from routed daily streamflow averaged over the season of interest from VIC model output for 1975–2004. We selected T (1, 3, and 5°C) and P (−10%, +1%, +10%, and +20%) perturbations that spanned the range of regional ΔT_{GCM} (y axis) and ΔP_{GCM} (x axis) projected by the CMIP5 GCMs in the mid-21st century (Figure 1).

We demonstrate the technique in three watersheds (Figure S1) that represent different types of hydrology and have somewhat different management challenges: (1) the Willamette Basin, with rain-dominated hydrology and peak flows in fall or winter, where we focused on June–August streamflow, a season when low flows stress farmers and fish [*Jaeger et al*., 2013], (2) the Yakima River basin, an agriculture-rich region with mixed snow-rain hydrology (rain-fed peak in fall-winter and snowmelt peak in spring), where we focused on the irrigation season of April–September [*USBR*, 2002], and (3) the Columbia Basin headwaters that have snow-dominated hydrology (flows peak in about June), where we focused on April–June streamflow, the period of greatest snowmelt [*Federal Columbia River Power System*, 2001].

2.2.2. Vegetation Carbon Sensitivities

We calculated annual vegetation carbon sensitivities (S_c, ε_c) using MC2, a dynamic general vegetation model that simulates, with the monthly time step, the biogeochemical response of plant functional types to climate conditions and includes the occurrence of fire. We configured MC2 to run from 1895 to 2009 at 1/24° resolution using PRISM climate data [*Daly et al*., 2008] and STATSGO-based soil data set [*Kern*, 1995]. We calibrated MC2 to approximate potential natural vegetation [*Küchler*, 1964] and the mean fire return interval for major vegetation types [*Leenhouts*, 1998]. MC2 calculates monthly live vegetation carbon and outputs annual averages. We applied T and P perturbations to the input climate data every month of the year and calculated S_c (equation (1)) and ε_c (equation (2)) of total live vegetation carbon average from 1970 to 1999. We used perturbations of T (1, 2, 3, 4, 5, and 6°C) and P (−10%, −5%, +1%, +5%, +10%, and +20%) that span the range of regional ΔT_{GCM} (y axis) and ΔP_{GCM} (x axis).

We evaluated vegetation response in three Bailey ecoregions [*Bailey*, 1983] in the PNW. These vegetation carbon responses vary throughout the season and are less predictably seasonally accentuated (versus seasonal responses as with hydrology); therefore, to adequately capture the vegetation response to climate change that occurs in multiple seasons, we focus on annual responses. All three ecoregions experience generally wet winters and dry summers, with moderate temperatures throughout the year except for the high elevation areas of the Western Cascades. These ecoregions lie on a humid-to-dry transect from west to east:

1. The Oregon and Washington (OR/WA) Coast Ranges, where Douglas fir (*Pseudotsuga menziesii*), redcedar (*Thuja plicata*), and western hemlock (*Tsuga heterophylla*) form dense conifer forests with typically plentiful soil water. Fires are infrequent, and cool temperatures slow bacterial activity.
2. The Western Cascades ecoregion is composed of uplifted sequences of volcanics and volcanoclastic rocks, with elevation ranging from near sea level to peaks higher than 4000 m. Soils are generally rich in organic matter and typically have plentiful soil water. Douglas fir and western hemlock dominate natural vegetation. Fire frequency is highly variable.
3. The Columbia Basin ecoregion is a high plain with loess hills and many scablands and shallow soils. Sagebrush (*Artemisia* spp.) and several species of bunch grasses dominate the vegetation. The fire regime has been shifting from frequently occurring small, stand-replacing fires to larger fires because of suppression and invasive grasses.

2.3. GCM Ranking

The ability of GCMs to reproduce observed climate can be quantified in many ways, and model ranking depends upon aspects of the climate analyzed and analysis methods [e.g., *Brekke et al*., 2008; *Pierce et al*., 2009; *Rupp et al*., 2013]. For each watershed and ecoregion, we used the evaluation by *Rupp et al*. [2013], who ranked GCMs from CMIP5 based on numerous metrics of the twentieth century climate of the PNW and surrounding area. Note that by ranking models by past performance, we assume that there is a connection between past and future performances—that is, in general, GCMs that better reproduce observed climate are likely to better simulate the future response to changing forcings. This assumption is a necessary, but not sufficient, condition for future accuracy that cannot be tested.

3. Results and Discussion

3.1. ΔT_{GCM} and ΔP_{GCM}

Figures 1 and 2 show the distribution of changes in ΔT_{GCM} and ΔP_{GCM} in each watershed and ecoregion of 142 projections from 33 individual GCMs, including two emission scenarios and multiple runs for some GCMs. Between study areas, GCMs have similar relative positions in ΔP-ΔT space, but GCMs generally project more warming and greater precipitation increases further north and further inland, indicating that ΔT_{GCM} and ΔP_{GCM} should be calculated close to the scale of the study area (e.g., Willamette Basin).

3.2. Impact-Relevant GCM Selection

The impact-relevant sensitivities are used to generate isolines of constant change that reflect the response surface of the relative influence of ΔT and ΔP on streamflow magnitude (Figure 1) or vegetation carbon (Figure 2). Through simultaneously considering the position on the impact spectrum, as defined by the isolines (e.g., high, medium, and low streamflow change), and GCM performance (i.e., lowest numbered GCMs are the best performing), a subset of GCMs can be easily identified that appropriately represent the range of possible futures and perform well relative to other GCMs.

Additionally, isolines also show how projections with different ΔT_{GCM} and ΔP_{GCM} compare to one another in terms of the impact. For instance, GCM projections might have similar streamflow declines, but for different reasons (e.g., in one projection a ΔP_{GCM} decrease combines with a small ΔT_{GCM} increase to give the same result as a projection where a ΔP_{GCM} increase is offset by a large ΔT_{GCM} increase).

3.2.1. Streamflow

The differences in response surfaces (isolines) between watersheds are influenced by both location and time of year (Figure 1) as determined by the watershed's seasonal hydrologic sensitivities (S_q, ε_q) (Figures 3a and 3b). For example, in Figure 1a, isolines indicate that increases in annual ΔT influence summertime streamflow in the Willamette up to 3°C, whereas between 3 and 5°C the temperature contribution (i.e., $S_q(\Delta T)\Delta T$) changes little and streamflow change is primarily driven by changing ΔP (vertical isolines). Similarly, streamflow for the irrigation season in the Yakima is influenced more by increasing ΔT for values less than 4°C. In both watersheds, S_q values become less negative per °C when calculated with larger ΔT (Figure 3a). Notably, this is a per °C change; with larger temperature increments, streamflow per °C decreases, primarily from earlier snowmelt but also from increased evapotranspiration. For larger ΔT, however, the rate of change becomes less per °C as there is less snow to melt and it is melting earlier. In the Willamette, for example,

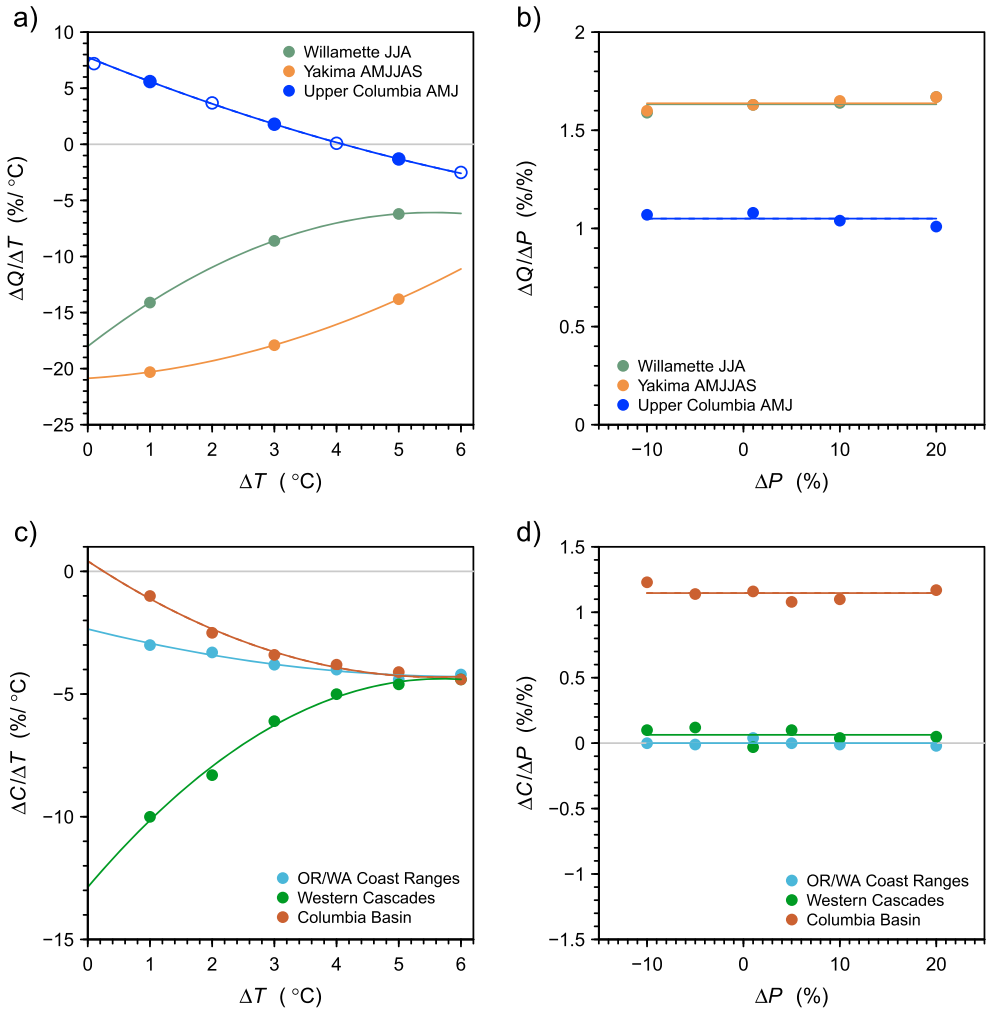

Figure 3. Hydrologic sensitivities for specified times of year for (a, b) three watersheds and annual vegetation carbon sensitivities for (c, d) three ecoregions calculated with increasing ΔT (Figures 3a and 3c) and ΔP (Figures 3b and 3d) perturbations. See Table S5 for values and curve fitting equation coefficients. This information is used to generate the isolines in Figures 1 and 2.

hydrographs with 3°C and 6°C perturbation increases are nearly identical because the watershed has little snow historically and with a 3°C increase practically all the snow is gone.

In the Upper Columbia, by contrast, the influence of T can increase (for $\Delta T \leq 4$°C) or decrease (for $\Delta T > 4$°C) springtime streamflow (Figure 1c). This is because we evaluated S_q in the spring when there is abundant snow to melt. With warming up to 4°C, streamflow in April–June increases because the hydrograph is shifting earlier (more spring snowmelt), but for warming greater than 4°C the seasonal shift is large enough (more snowmelt occurring before April) that even spring streamflow declines, resulting in the change from positive to negative S_q values (Figure 3a).

Seasonal temperature sensitivities (S_q) depend strongly on ΔT; therefore, when calculating the isolines, we used S_q values that changed as a function of ΔT according to the curves in Figure 3a. For our study's watersheds, the type of curve fitting (e.g., linear versus quadratic) makes little difference when calculating $S_q(\Delta T)$ as long as values are not extrapolated beyond the range of ΔT_{GCM} being evaluated (Figure 1, y axis). We found that calculating the change at 2°C increments (i.e., 1, 3, and 5°C) was sufficient; when the same evaluation was made at 1°C increments (i.e., 0.1, 1, 2, 3, 4, 5, and 6°C) in the Upper Columbia, smaller increments made no notable difference (Figure 3a). However, smaller increments would be important to evaluate if the curve were highly nonlinear and indicated strong threshold behavior. Seasonal precipitation

elasticities (ε_q) changed little with ΔP (Figure 3b); therefore, we assumed a linear P response and applied a constant ε_q value calculated as an average of the four perturbations.

We varied T and P independently, which assumes no interactions between effects of T and P. For small ΔT and ΔP throughout the PNW, we found little interactions, similar to *Vano et al.* [2012], and therefore did not pursue further analysis. However, one could vary T and P simultaneously, using, for example, Latin hypercube sampling, to efficiently select ΔT and ΔP pairs in a more thorough sensitivity analysis.

We used annual instead of seasonal changes in ΔT_{GCM} and ΔP_{GCM} from GCMs, but only after comparisons indicated similar streamflow responses with change calculated with seasonal ΔT_{GCM} and ΔP_{GCM}. In the PNW, streamflow is driven by seasonal T and P, where ΔT and ΔP have more influence in certain seasons depending on a watershed's hydrology [*Vano et al.*, 2015]. For example, seasonal hydrologic sensitivities in the Willamette calculated with nine separate VIC model simulations using one historical and four 3 month season perturbations for both T and P indicate that October–June temperatures and January–June precipitation contribute most to June–August streamflows. We tested how ΔT_{GCM} and ΔP_{GCM} in these influential seasons resulted in streamflow change that differed from annual ΔT_{GCM} and ΔP_{GCM} (see Text S1). We found that this additional step had little influence on the overall position of individual GCMs on the ΔP-ΔT plots, largely because there were high correlations between the seasons of influence (e.g., October–June temperatures in the Willamette) and annual changes. Therefore, to keep the analysis consistent, we used annual ΔT_{GCM} and ΔP_{GCM} values.

3.2.2. Vegetation Carbon

As with hydrology, in all ecoregions vegetation carbon temperature sensitivities (S_c) varied substantially across ΔT perturbations (Figure 3c), while vegetation carbon precipitation elasticities (ε_c) were nearly constant across ΔP values (Figure 3d). Therefore, we used S_c values that varied as a function of ΔT according to quadratic curves and assumed constant ε_c values (Table S5). We used more perturbations of ΔT and ΔP (smaller change increments) than with streamflow as the behavior initially appeared more nonlinear with potential thresholds. In retrospect, larger change increments/less perturbations would have given similar results.

The response of simulated vegetation carbon to ΔT and ΔP varies distinctly across the three ecoregions, where changes are either from ΔT alone or the combination of ΔT and ΔP. For example, responses in OR/WA Coast Ranges and Western Cascades are driven by ΔT, as reflected by the nearly horizontal isolines (Figures 2a and 2b) that are a result of small ε_c values, between 0 and −0.2% (Figure 3d). Therefore, a 3°C increase results in a reduction of ~10% in vegetation carbon in the OR/WA Coast Ranges and a ~20% reduction in the Western Cascades, regardless of ΔP. The OR/WA Coast Ranges ecoregion has fairly consistent S_c values, ranging from −3.0% to −4.4% per °C, whereas the Western Cascades has a relatively large S_c (10.0% per °C) with a 1°C perturbation, but values converge with OR/WA Coast Ranges for perturbations greater than 4°C (Figure 3c). The difference in S_c between these two ecoregions occurs because of fire (Figure S2): in the Western Cascades ecoregion, fire consumes 0.02% carbon during the historical period and 0.07% under the 6°C perturbation experiment. In the OR/WA Coast Ranges, despite plentiful fuels, fire increases less because abundant rainfall maintains high levels of fuel moisture, reducing the overall occurrence of simulated fires and fire effects.

In contrast, in the dry Columbia Basin both ΔT and ΔP affect vegetation carbon, which is reflected as slanted isolines in Figure 2c, where a +2°C ΔT can be offset by a +5% ΔP and a +3°C ΔT can be offset by a +10% ΔP (Figure 2). While simulated net primary productivity in the other two ecoregions is limited by T, simulated net primary productivity in the Columbia Basin is limited by available water. The average annual T of all ecoregions are similar, ranging from 9 to 11.5°C (1970–1999), but average annual P in the Columbia Basin is only 310 mm, compared to 2470 mm in OR/WA Coast Ranges. When we increase P in the Columbia Basin by more than 10%, the robust response in primary productivity shifts the vegetation from a grassland ecosystem into a woodland ecosystem (Figure S3).

3.3. Impact Distributions

This approach can also be used to quickly generate histograms that estimate, using equation (3), the distribution of all GCM responses, and this can be done separately for the two emission scenarios (Figure 4). This back-of-the-envelope approach is similar to estimates of streamflow change in *Vano and*

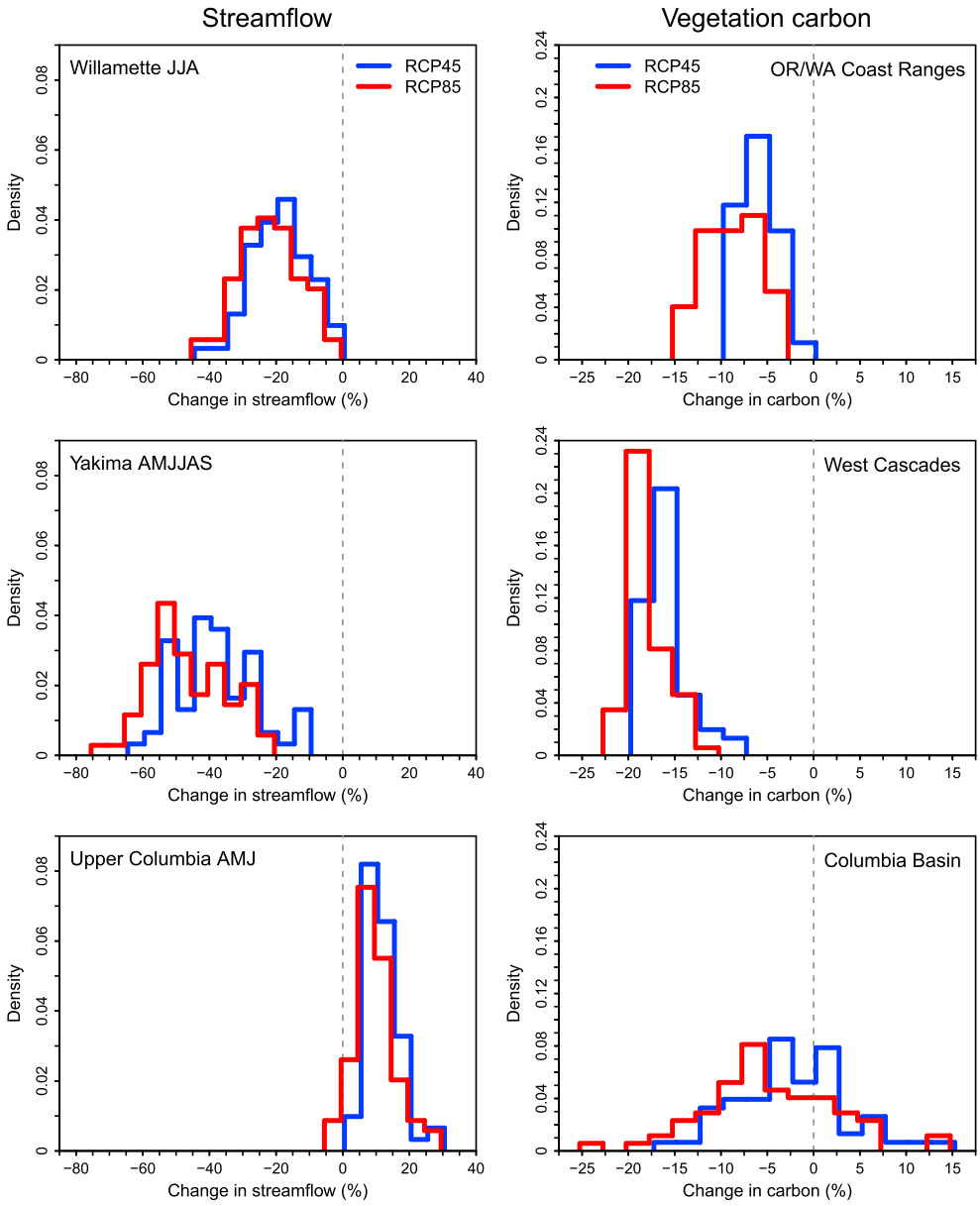

Figure 4. Impact distributions calculated with ΔT_{GCM} and ΔP_{GCM} from all GCMs for (left column) streamflow and (right column) vegetation carbon change.

Lettenmaier [2014], though here we use annual ΔT_{GCM} and ΔP_{GCM} that are not weighted by monthly values. These histograms place the response for an individual GCM in context with the responses of the full ensemble.

As a complement to detailed impacts modeling, this approach provides a clear view of the range and probability distribution of possible outcomes, which is frequently desired by management agencies. For example, these histograms reveal the relative differences in how higher (RCP8.5) versus lower (RCP4.5) emissions affect streamflow magnitude and vegetation carbon. In all watersheds and ecoregions, higher emissions, on average, result in greater declines in both streamflow magnitude and vegetation carbon. Additionally, with vegetation carbon change, all responses are calculated on an annual basis and differences between ecoregions are entirely because of location (versus season and location as in watersheds). As such, the histograms highlight that carbon changes are projected to be greatest in the Western Cascades and most varied in the Columbia Basin ecoregion.

4. Conclusions

We outline an efficient approach to help impact researchers and natural resource managers more effectively use GCM information. The approach, through impact model evaluation, provides an estimate of the magnitude of change of a particular impact (e.g., summertime streamflow) from climate change projections prior to detailed multimodel analysis. These estimates provide a judicious, defensible evaluation structure that can be used to select a subset of GCMs for further analysis, as well as probability distributions of future changes for different emission scenarios. The evaluation structure employs isolines (as in Figures 1 and 2, generated through a sensitivity analysis) and a ranking of GCM performance to select climate change projections that (1) appropriately represent the range of potential impacts and (2) adequately simulate regional climate.

In our analysis, which methodically evaluates how changes in T and P affect the impact of interest, we found that S varied as a function of T increases, whereas ε remained relatively constant for varying magnitudes of P change. Therefore, when generating isolines, we held one variable (ε) constant while varying the other (S). We do not anticipate that this will always be true in other locations and for other impacts, especially when the range of ΔT_{GCM} and ΔP_{GCM} increases. When a simplifying assumption does not apply, both variables can be varied simultaneously.

This approach is advantageous because of the following:

1. It allows the impact of interest to guide GCM selection rather than just selecting GCMs with large and/or small ΔT_{GCM} and ΔP_{GCM}.
2. It is computationally efficient. In this study we evaluated 142 future GCM scenarios using just eight simulations from the hydrology impact model and 13 simulations from the vegetation carbon impact model. Once calculated, impact sensitivities can be used with any future projections and only need to be recalculated to update the historical period (recommended if historical temperatures changed significantly, e.g., by 3°C), changes in land cover, or to incorporate improvements in the impact model (e.g., updated hydrologic model parameterization).
3. It is resource efficient. The simple-to-set-up perturbation experiments provide insights into understanding the nature of changes, e.g., the influence of changes in T versus P.
4. It selects representative GCMs for further investigation, which reduces data management needs and the time needed to process data provided that GCM rankings exist and impacts can be assessed accurately enough using through long-term annual ΔP and ΔT (not extremes). In each region, we selected a single impact. In cases when there are multiple factors (e.g., both streamflow and vegetation carbon), isolines could be superimposed. Then to appropriately represent the range of impacts, more than three GCMs could be selected.
5. It is transferable. We demonstrate the approach for two impacts using a single hydrologic model and single vegetation model, but this approach could be applied using other simulation models or potentially other impacts.

Acknowledgments
The authors thank two anonymous reviewers for their feedback and G. Stephen Pitts for technical assistance with running MC2 simulations. GCM precipitation and temperature changes were calculated from data downloaded at http://cmip-pcmdi.llnl.gov/cmip5. This material is based upon the work supported by the National Science Foundation (NSF) under awards EAR-1250087 and EAR-1039192, by the U.S. National Oceanic and Atmospheric Administration (NOAA), grant NA10OAR4310218, and by the Department of the Interior Northwest Climate Science Center (NW CSC) through a cooperative agreement (G12AC20495) from the United States Geological Survey (USGS). Its contents are solely the responsibility of the authors and do not necessarily represent the views of the NSF, NOAA, NW CSC, or the USGS. This manuscript is submitted for publication with the understanding that the United States Government is authorized to reproduce and distribute reprints for governmental purposes.

The Editor thanks two anonymous reviewers for their assistance in evaluating this paper.

References

Adelsman, H., and J. Ekrem (2012), Preparing for a Changing Climate: Washington State's Integrated Climate Response Strategy, Washington Department of Ecology, Publication No. 12-01-004, Olympia, Wash. [Available at http://www.ecy.wa.gov/climatechange/ipa_responsestrategy.htm.]

Adger, N. W., N. W. Arnell, and E. L. Tompkins (2005), Successful adaptation to climate change across scales, *Global Environ. Change*, *15*(2), 77–86.

Bailey, R. G. (1983), Delineation of ecosystem regions, *Environ. Manage.*, *7*(4), 365–373.

Brekke, L. D., M. D. Dettinger, E. P. Maurer, and M. Anderson (2008), Significance of model credibility in estimating climate projection distributions for regional hydroclimatological risk assessments, *Clim. Change*, *89*, 371–394.

Brown, C., and R. L. Wilby (2012), An alternate approach to assessing climate risks, *Eos Trans. AGU*, *93*(41), 401, doi:10.1029/2012EO410001.

Daly, C., M. Halbleib, J. I. Smith, W. P. Gibson, M. K. Doggett, G. H. Taylor, J. Curtis, and P. P. Pasteris (2008), Physiographically sensitive mapping of climatological temperature and precipitation across the conterminous United States, *Int. J. Climatol.*, *28*(15), 2031–2064.

Elsner, M. M., L. Cuo, N. Voisin, J. S. Deems, A. F. Hamlet, J. A. Vano, K. E. B. Mickelson, S. Y. Lee, and D. P. Lettenmaier (2010), Implications of 21st century climate change for the hydrology of Washington State, *Clim. Change*, *102*(1), 225–260.

Federal Columbia River Power System (2001), *The Columbia River System Inside Story: Federal Columbia River Power System*, 2nd ed., Bonneville Power Administration, Portland, Oreg.

Giorgi, F., and L. Mearns (2002), Calculation of average, uncertainty range, and reliability of regional climate changes from AOGCM simulations via the "reliability ensemble averaging" (REA) method, *J. Clim.*, *15*, 1141–1158.

Hamlet, A. F., M. M. Elsner, G. S. Mauger, S. Y. Lee, I. Tohver, and R. A. Norheim (2013), An overview of the Columbia Basin Climate Change Scenarios Project: Approach, methods, and summary of key results, *Atmos. Ocean*, *51*(4), 392–415, doi:10.1080/07055900.2013.819555.

Harding, B. L., A. W. Wood, and J. R. Prairie (2012), The implications of climate change scenario selection for future streamflow projection in the Upper Colorado River Basin, *Hydrol. Earth Syst. Sci.*, *16*, 3989–4007, doi:10.5194/hessd-16-3989-2012.

Jaeger, W. K., et al. (2013), Toward a formal definition of water scarcity in natural-human systems, *Water Resour. Res.*, *49*, 4506–4517, doi:10.1002/wrcr.20249.

Kern, J. S. (1995), Geographic patterns of soil water-holding capacity in the contiguous USA, *Soil Sci. Soc. Am. J.*, *59*, 1126–1133.

Küchler, A. W. (1964), *Potential Natural Vegetation of the Conterminous United States*, vol. 36, Am. Geogr. Soc., New York.

Leenhouts, B. (1998), Assessment of biomass burning in the conterminous United States, *Conserv. Ecol.*, *2*(1), 1.

Liang, X., D. P. Lettenmaier, E. F. Wood, and S. J. Burges (1994), A simple hydrologically based model of land surface water and energy fluxes for general circulation models, *J. Geophys. Res.*, *99*, 14,415–14,428, doi:10.1029/94JD00483.

Means, E., M. Laugier, J. Daw, L. Kaatz, and M. Waage (2010), Decision support planning methods: Incorporating climate change uncertainties into water planning Water Utility Climate Alliance. [Available at www.wucaonline.org.]

Meinshausen, M., et al. (2011), The RCP greenhouse gas concentrations and their extensions from 1765 to 2300, *Clim. Change*, *109*, 213–241.

Mote, P. W., and E. P. Salathé Jr. (2010), Future climate in the Pacific Northwest, *Clim. Change*, *102*, 29–50.

Mote, P. W., L. Brekke, P. B. Duffy, and E. Maurer (2011), Guidelines for constructing climate scenarios, *Eos Trans. AGU*, *92*(31), 257, doi:10.1029/2011EO310001.

Pierce, D. W., T. P. Barnett, B. D. Santer, and P. J. Gleckler (2009), Selecting global climate models for regional climate change studies, *Proc. Natl. Acad. Sci. U.S.A.*, *106*, 8444–8446.

Pitman, A. J., and S. E. Perkins (2008), Regional projections of future seasonal and annual changes in rainfall and temperature over Australia based on skill-selected AR4 models, *Earth Interact.*, *12*, 1–50, doi:10.1175/2008EI260.1.

Rupp, D. E., J. T. Abatzoglou, K. C. Hegewisch, and P. W. Mote (2013), Evaluation of CMIP5 20th century climate simulations for the Pacific Northwest USA, *J. Geophys. Res. Atmos.*, *118*, 10,884–10,906, doi:10.1002/jgrd.50843.

Snover, A. K., N. J. Mantua, J. S. Littell, M. A. Alexander, M. M. Mcclure, and J. Nye (2013), Choosing and using climate-change scenarios for ecological-impact assessments and conservation decisions, *Conserv. Ecol.*, *27*(6), 1147–1157.

Taylor, K. E., R. J. Stouffer, and G. A. Meehl (2012), An overview of CMIP5 and the experiment design, *Bull. Am. Meteorol. Soc.*, *93*, 485–498, doi:10.1175/BAMS-D-1100094.1.

U.S. Bureau of Reclamation (USBR) (2002), *Interim Comprehensive Basin Operating Plan for the Yakima Project, Washington*, Yakima Field Office, Yakima, Wash.

U.S. Bureau of Reclamation (USBR) (2013), Colorado River basin water supply and demand study, Final Study Reports, U.S. Dep. of the Interior, Boulder, Nevada. [Available at http://www.usbr.gov/lc/region/programs/crbstudy/finalreport/index.html, accessed 9 June 2014.]

U.S. Environmental Protection Agency (2009), A framework for categorizing the relative vulnerability of threatened and endangered species to climate change, National Center for Environmental Assessment, Washington, D. C., National Technical Information Service, Springfield, Va. [Available at http://www.epa.gov/ncea.]

U.S. Fish and Wildlife Service (2013), National fish, wildlife, and plants climate adaptation strategy. [Available at http://www.wildlifeadaptationstrategy.gov.]

Vano, J. A., and D. P. Lettenmaier (2014), A sensitivity-based approach to evaluating future changes in Colorado River discharge, *Clim. Change*, *122*(4), 621–634, doi:10.1007/s10584-013-1023-x.

Vano, J. A., T. Das, and D. P. Lettenmaier (2012), Hydrologic sensitivities of Colorado River runoff to changes in precipitation and temperature, *J. Hydrometeorol.*, *13*, 932–949, doi:10.1175/JHM-D-11-069.1.

Vano, J., B. Nijssen, and D. P. Lettenmaier (2015), Seasonal hydrologic responses to climate change in the Pacific Northwest, *Water Resour. Res.*, *51*(4), doi:10.1002/2014WR015909.

Weaver, C. P., R. J. Lempert, C. Brown, J. A. Hall, D. Revell, and D. Sarewitz (2013), Improving the contribution of climate model information for decision making: The value and demands of robust decision frameworks, *WIREs Clim. Change*, *4*, 39–60, doi:10.1002/wcc.202.